JJMIE

Volume 13, Number 4, December. 2019
ISSN 1995-6665
Pages 253 - 264

Jordan Journal of Mechanical and Industrial Engineering

Three-Material Beam: Experimental Setup and Theoretical Calculations

Mohammad A. Gharaibeh[a], Adel A. Ismail, Ahmad F. Al-Shammary, Omar A. Ali

Mechanical Engineering Department, The Hashemite University, Az Zarqa 13133, Jordan

Received 19 August. 2019

Abstract

This paper presents an experimental setup for the evaluation of the lateral deflection of a three-material composite beam subjected to a concentrated force. The three materials used in this setup are steel, aluminum and wood. In this experiment, two layer-bonding methods were considered: glued and bolted. In the glued configurations, the three stacked up layers were attached to each other using glue commercial along the beam length. For the bolted system, the layers were connected using four symmetrically-distributed bolts and nuts. The experimental results of the beam lateral deflections, for both bonding methods, were compared to theoretical computations. Comparison results showed that the glued system deflection data were in better agreement with theory. Also in this paper, the equivalent section method was implemented to solve for the composite beam bending stresses. Finally, the effect of the key geometric and material parameters of the composite beam on the beam bending stress is thoroughly investigated with the emphasis on the structural analysis of electronic assemblies subjected to mechanical bending loading.

Keywords: Three-Material Beams, Electronic Packaging, Experiments, Theory.

1. Introduction

The problem of a beam composed of two or more materials appears in several real-life engineering applications such as the composite beams used in highway and building constructions [1] as well as in electronic packaging industry [2]. For building constructions, composite beams are usually made of concrete slabs that are re-enforced by steel bars joined by mechanical connectors or epoxy resins [3, 4]. In electronics, a typical electronic system consists of a printed circuit board (PCB), an integrated circuit (IC) component both are connected by solder interconnects. The three-material beam problem has been successfully used to model this electronic structure [5]. For this problem, several elasticity solutions were presented and related to the electronic packaging application [6-8]. For experimental work, only a few papers were published in the area of the experimental evaluation of composite beam structures [9-11].

A larger scale problem that has been widely studied in the electronic packaging application, is the multi-layer plates. In 2015, Gharaibeh et al. [12] provided an analytical solution based on Ritz method to solve for the natural frequencies, mode shapes and the dynamic response of an elastically-coupled plates system. This analytical model was validated with finite element simulations and with experiments. Hence, this solution was employed to study the effect of the various geometric and material parameters of the electronic system on the stresses, i.e. fatigue performance, of the assembly. This assembly was further expanded to solve for the transient and random vibration responses of electronic structures [13-17].

In addition to electronics application, the composite beam structure is widely used in the microelectromechanical systems (MEMS). Ghadiri et al. [18] investigated the effect of the non-ideal supports on the free vibration of composite beams with spring-mass-damper attachments analytically. The study results showed that the arrangements of the layers of the composite beams as well as the support uncertainty could significantly affect the natural frequencies and the out-of-plane deformations of the composite beam structure. Sari et al. [19] studied the non-linear dynamic response of a composite beam with initial imperfections between the beam layers using the nonlocal elasticity theory. They proved that such type of imperfections have a non-negligible effect on the beam linear as well as nonlinear behaviors.

The objective of this paper is to provide an experimental setup for the evaluation of the lateral deflections of a three-material composite beam subjected to a concentrated point force. In this setup, two methods were used to bond the three layers of the composite structure. The experimentally measured beam deflections were validated with theory. In addition, this paper

* Corresponding author e-mail: mohammada_fa@hu.edu.jo

presented a thorough discussion, based on mechanics of materials analytical solution, on the effect of the key parameters of the composite beam on the structural analysis of electronic assemblies under mechanical bending.

2. Description of the Problem

The three-material beam structure can be defined as a beam consisting of three material layers stacked up and joined together, as shown in Figure 1(a). Specifically, this beam is made of the top layer (layer 1), the middle layer (layer 2) and the bottom layer (layer 3). In the present analysis, the three layers are considered to have identical lengths (L) and widths (b). The top, middle and bottom layers are selected to be ST37 Steel, T6061 Aluminum and commercial wood, respectively. The geometric details and material properties of this structure are listed in Table 1.The beam of the present analysis is considered to beam simply supported at both ends and loaded by a concentrated point force (P) at a distance x from the left end, as shown in Figure 1(b).

Table 1. Geometric and material properties of the three-material beam.

Beam layer #	Material	Thickness	Width	Length	Elastic Modulus
Top (1)	ST37 Steel	$h_1 = 10\ mm$	$b = 300\ mm$	$L = 1\ m$	$E_1 = 200\ GPa$
Middle (2)	T6061 Aluminum	$h_2 = 10\ mm$			$E_2 = 70\ GPa$
Bottom (3)	Wood	$h_3 = 10\ mm$			$E_3 = 13\ GPa$

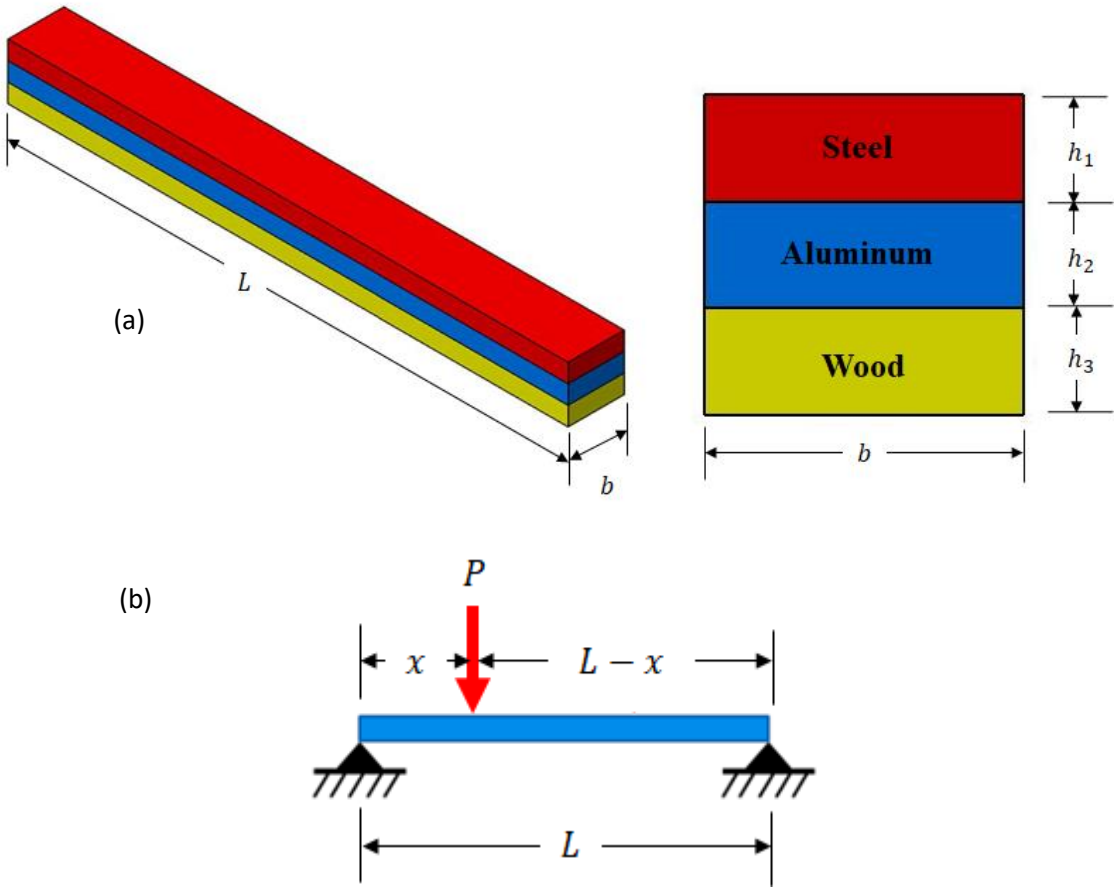

Figure 1. (a) Three-material beam configuration (b) Simply supported beam with point force.

3. Mathematical Modeling

Equivalent section method is a common solution approach used to solve for the bending deflections, strains and stresses of composite beams. The chief assumption of this method is that the axial strain is linearly proportional throughout the beam cross section, irrespective of material. For a three-material composite beam, this method aims to transform an existing two materials to one material with an equivalent cross section. Generally, the width of the stiffer material is increased by the ratio of the elastic moduli to calculate the transformed section moment of inertia. Conversely, the width of the softer material is reduced to provide the equivalent section. In both cases, the thickness of each layer remains unchained due to the previously mentioned assumption. In this paper, the steel and aluminum layers are mathematically transformed to wood. Thus, the ratio between steel and wood (n_1) and aluminum to wood (n_2) elastic moduli are given by

$$n_1 = \frac{E_1}{E_3} \quad (1.a)$$

$$n_2 = \frac{E_2}{E_3} \quad (1.b)$$

Therefore, the width of steel (b_s) and aluminum (b_a) in the transformed section would be

$$b_s = bn_1 \quad (2.a)$$

$$b_s = bn_2 \quad (2.b)$$

Thus, the centroidal axis location measured from the beam bottom ($\bar{y}$) and the moment of inertia about the centroidal axis (I) are given by

$$\bar{y} = \frac{n_1 h_1(0.5h1 + h_2 + h_3) + n_2 h_2(0.5h_2 + h_3) +}{n_1 h_1 + n_2 h_2 + h_3} \quad (3)$$

$$\begin{aligned} I = b\Big(&\frac{1}{12}n_1 h_1^3 + n_1 h_1(0.5h_1 + h_2 + h_3 - \bar{y})^2 \\ &+ \frac{1}{12}n_2 h_2^3 \\ &+ n_2 h_2(0.5h_2 + h_3 - \bar{y})^2 \\ &+ \frac{1}{12}h_3^2 + h_3(0.5h_3 - \bar{y})^2\Big) \end{aligned} \quad (4)$$

Now, the lateral deflection of the beam at the force location $y(x)$ can be easily calculated as

$$y(x) = -\frac{PL^3}{48E_3 I}(3L^2 - 4x^2) \quad (5)$$

Where $0 \le x \le L/2$.

The results of the experimentally measured deflections for different beam configurations will be validated with Eq. (5) above.

4. Experimental Setup

The experimental setup used to measure the composite beam lateral deflection in this work is shown in Figure 2. This setup includes test fixture, beam supports and load application handle as well as the composite beam test piece. The beam lateral deflection was measured using a high accuracy dial gage with a precision of $0.001mm$. Also, the concentrated force was applied by placing masses on the load application handle. Masses (M) of 1, 2, 3 5, 6 and 8 kilograms were used in this experiment. The point force was then calculated using simple equation $\mathrm{P = Mg}$ where g is the gravity acceleration and equal to $9.81\ \mathrm{m/s^2}$. To eliminate the handle effect, the dial gage was zeroed after placing the load application handle on the beam body. The beam deflection was measured at three different locations $x = 200, 300$ and $500\,mm$ while the load is applied on the beam center point ($L/2$). For each test run, three trials were made and then the mean value of the three trials was used as a final data point.

Two beam joining methods were tested in this work; glued and bolted beam configurations. For the glued configuration, the three layers were joined together using a thin layer of ALTECO110 high strength Cyanoacrylate adhesive. Care was taken to ensure equal glue deposition along the beam length. For the bolted system, the beam layers were attached by four symmetrically-distributed bolts and held by washers and nuts.

5. Results and Discussions

5.1. Experimental Results

The experimental results of the previously discussed loading conditions from both beam configurations were collected and compared to theoretical calculations of Eq. (5). The results of this comparison are listed in Table 2 and Table 3.

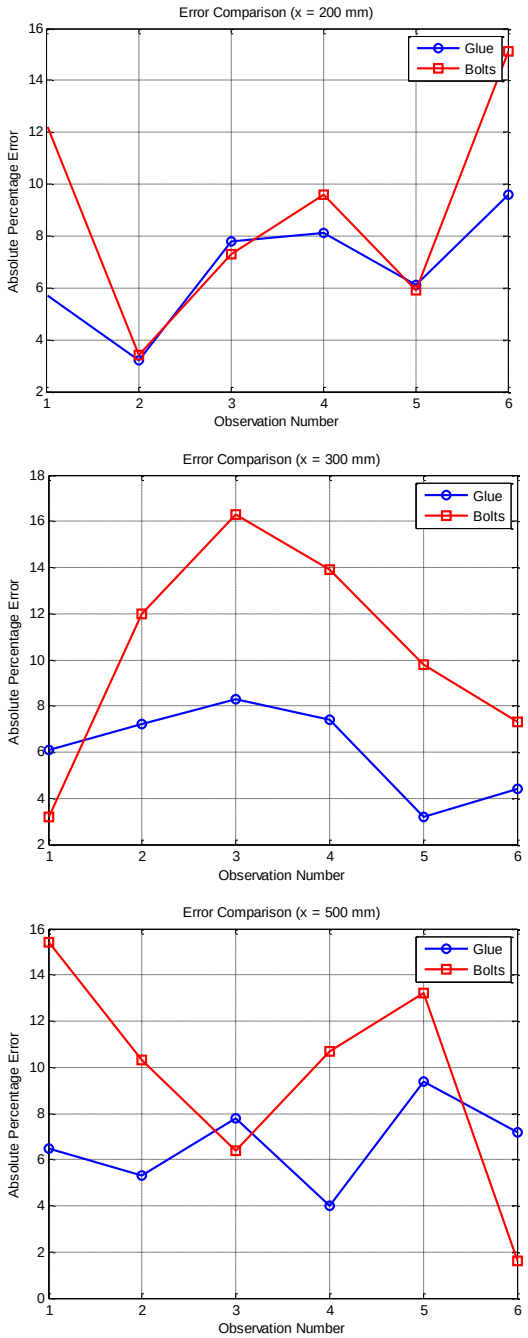

Figure 3. Error comparison between glued and bolted beam configurations for different loading locations.

Table 2. Lateral deflection results for the glued beam configuration.

$x = 200mm$					
Observation #	**M (kg)**	**P (N)**	**Experiment (mm)**	**Theory (mm)**	**% Error**
1	1	9.81	0.032	0.034	5.7
2	2	19.62	0.066	0.068	3.2
3	3	29.43	0.110	0.102	-7.8
4	5	49.05	0.156	0.169	8.1
5	6	58.86	0.216	0.203	-6.1
6	8	78.48	0.245	0.271	9.6
$x = 300mm$					
1	1	9.81	0.044	0.047	6.1
2	2	19.62	0.101	0.094	-7.2
3	3	29.43	0.153	0.142	-8.3
4	5	49.05	0.219	0.236	7.4
5	6	58.86	0.274	0.283	3.2
6	8	78.48	0.361	0.378	4.4
$x = 500mm$					
1	1	9.81	0.056	0.060	6.5
2	2	19.62	0.113	0.119	5.3
3	3	29.43	0.197	0.179	-10.2
4	5	49.05	0.310	0.298	-4
5	6	58.86	0.324	0.358	9.4
6	8	78.48	0.443	0.477	7.2

From both tables, it can be seen that both beam configurations experimental results are in well agreement with theoretical calculations with a percentage error of less than 11% in the glued configuration and less than 17% in the bolted system. However, the errors in the bolted configuration are observed to be higher than those of the glued system. This observation is confirmed in **Figure 3**. This means that the glued system models this problem experimentally better than the bolted system and that is due to the fact that the glue provides very low stiffness along the beam length unlike the high local stiffness at bolts locations in the bolted system.

Figure 2. Experimental setup (a) main frame (b) dial gage.

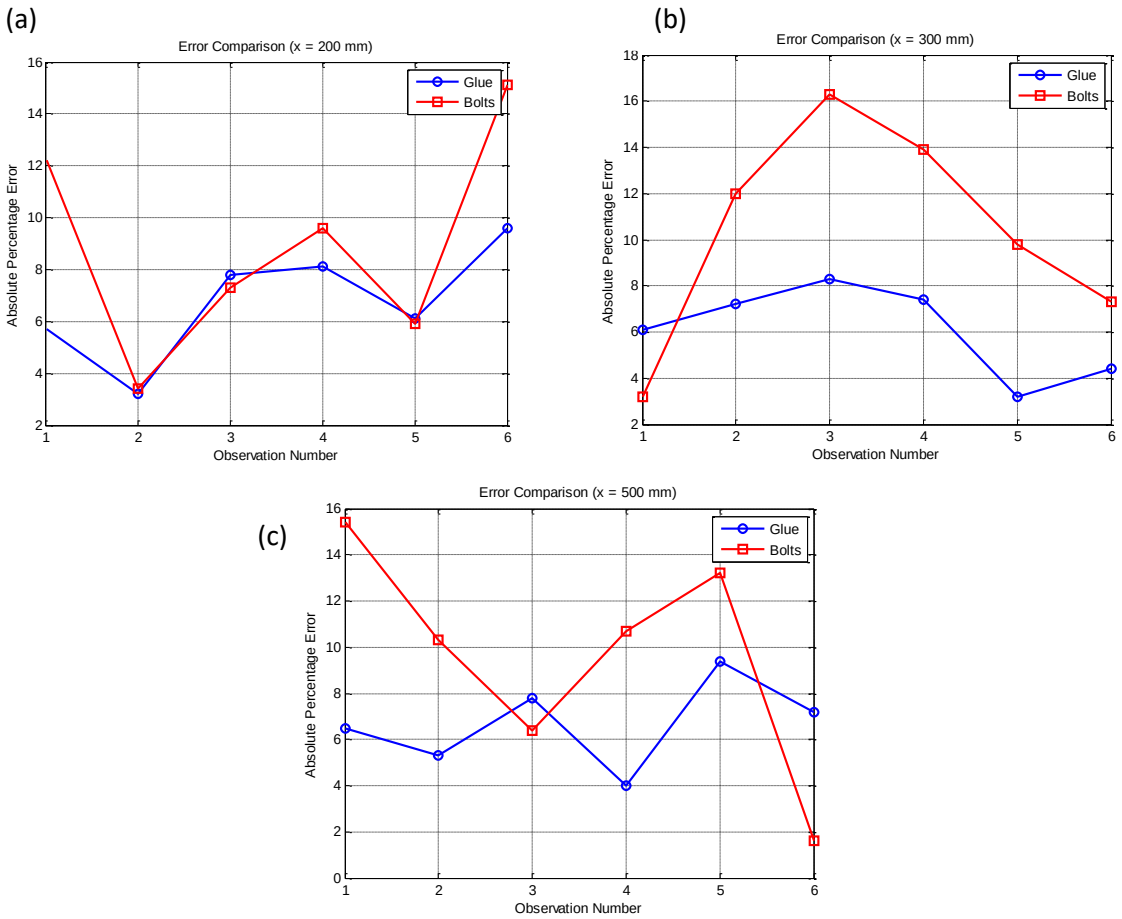

Figure 3. Error comparison between glued and bolted beam configurations for different loading locations.

Table 2. Lateral deflection results for the glued beam configuration.

$x = 200mm$					
Observation #	**M (kg)**	**P (N)**	**Experiment (mm)**	**Theory (mm)**	**% Error**
1	1	9.81	0.032	0.034	5.7
2	2	19.62	0.066	0.068	3.2
3	3	29.43	0.110	0.102	-7.8
4	5	49.05	0.156	0.169	8.1
5	6	58.86	0.216	0.203	-6.1
6	8	78.48	0.245	0.271	9.6
$x = 300mm$					
1	1	9.81	0.044	0.047	6.1
2	2	19.62	0.101	0.094	-7.2
3	3	29.43	0.153	0.142	-8.3
4	5	49.05	0.219	0.236	7.4
5	6	58.86	0.274	0.283	3.2
6	8	78.48	0.361	0.378	4.4
$x = 500mm$					
1	1	9.81	0.056	0.060	6.5
2	2	19.62	0.113	0.119	5.3
3	3	29.43	0.197	0.179	-10.2
4	5	49.05	0.310	0.298	-4
5	6	58.86	0.324	0.358	9.4
6	8	78.48	0.443	0.477	7.2

Table 3. Lateral deflection results for the bolted beam configuration.

$x = 200mm$					
Observation #	**M (kg)**	**P (N)**	**Experiment (mm)**	**Theory (mm)**	**% Error**
1	1	9.81	0.030	0.034	12.2
2	2	19.62	0.065	0.068	3.4
3	3	29.43	0.109	0.102	-7.3
4	5	49.05	0.153	0.169	9.6
5	6	58.86	0.215	0.203	-5.9
6	8	78.48	0.230	0.271	15.1
$x = 300mm$					
1	1	9.81	0.046	0.047	3.2
2	2	19.62	0.106	0.094	-12.0
3	3	29.43	0.119	0.142	16.3
4	5	49.05	0.269	0.236	-13.9
5	6	58.86	0.256	0.283	9.8
6	8	78.48	0.350	0.378	7.3
$x = 500mm$					
1	1	9.81	0.069	0.060	-15.4
2	2	19.62	0.107	0.119	10.3
3	3	29.43	0.177	0.179	1.3
4	5	49.05	0.330	0.298	-10.7
5	6	58.86	0.405	0.358	-13.2
6	8	78.48	0.470	0.477	1.6

5.2. Stress Analysis

The problem of three-material beam was extensively raised by engineers in electronic packaging industry. Typically, an electronic package consists of three common parts: The printed circuit board (PCB), solder interconnects area array and the integrated circuit (IC) component. Researchers in electronic packaging field, modeled this electronic structure using the three-material beam considering that the PCB is the bottom beam, the solder interconnects layer is the middle and finally the IC component is the top beam. Numerous research studies using elasticity solutions investigated the effect of the geometric and material characteristics of the electronic assembly on solder stresses as they are the most critical design factor. In the case of solder failure, it has been seen that the solder cracks are initiated at the top or the bottom (component and PCB sides, respectively) of the solder. Therefore, it is very important to investigate stress distributions at the both sides of the solder. In this paper, the previously presented method of equivalent section was used to compute the bending-induced solder stresses. Here, the stresses at the interface between the bottom and middle beams (PCB side) as well as between the top and the middle beams (component side) were investigated. Thus, the common bending stress in beams (σ) equation is expressed as:

$$\sigma = \frac{Mc}{I} \tag{6}$$

Where M is the bending moment, c is the vertical distance from the equivalent section centroidal axis and I is the moment of inertial of the equivalent section.

In the present analysis, the effect of the ratio between the thickness of the top beam and the thickness of the middle beam (h_1/h_2) and the ratio between the thickness of the bottom beam and the thickness of the middle beam

(h_3/h_2) on the middle beam stresses at interfaces with the top and bottom beams was studies and fully presented. Besides, this work examines the effect of the ratio between the elastic moduli of the top and middle beams (E_1/E_2) as well as the ratio elastic moduli of the bottom and middle beams (E_3/E_2). In electronic packaging words, ratios h_1/h_2 and h_3/h_2 represent the ratios of the thickness of the IC component and PCB to the solder joint standoff height. Also, ratios E_1/E_2 and E_3/E_2 represent the ratios of the elastic moduli of the IC component and PCB to the solder joint elastic modulus.

In the present analysis, Eq. (6) was used to evaluate middle beam interface stresses assuming a unity positive bending moment load ($M = 1$) and a beam width ($b = 1$). In this equation, the distance from the centroidal axis to the middle beam top surface is $c = h_2 + h_3 - \bar{y}$ and the distance from the centroidal axis to the middle beam bottom surface is $c = \bar{y} - h_3$. As the equivalent section in the present paper was created to be wood, the resultant stress of Eq. (6) was multiplied by the ratio between the middle beam and bottom beam elastic moduli ratio (n_2).

Figure 4shows the effect of E_1/E_2 on the middle layer top and bottom stresses. For the top surface stresses, the middle layer stresses to be very high for stiff middle layer ($E_1/E_2 \leq 1$). However, for softer layers ($E_1/E_2 \geq 1$), the top surface stress becomes lower and approaches to zero for very high E_1/E_2 ratios. For bottom surface stress, tensile stresses tend to increase as E_1/E_2 increase in the range of $0 \leq E_1/E_2 \leq 2$ at the case of equal elastic moduli of bottom and middle layers ($E_3/E_2 = 1$). For higher E_3/E_2 values, the bottom surface stresses start to be compressive then they transfer to be tensile stress for higher E_1/E_2 ratios. Therefore, it is highly recommended to design an electronic assembly with component to solder elastic moduli ratio between zero and 2 combined with PCB to solder elastic moduli ratio higher than 3.

Figure 5 and Figure 6 represent the effect of E_1/E_2 on the middle layer top and bottom stresses at different h_1/h_2 and h_3/h_2 ratios, respectively. in both cases, middle beam top stresses are observed to be higher for small E_1/E_2 values while they eventually dying out for high ratios. Additionally, bottom surface stresses are very high for a unity h_1/h_2 and h_3/h_2 ratios. Besides, bottom surface stresses are higher in the range of $E_1/E_2 \leq 2$ while much lower stresses appear for high E_1/E_2 configurations. Therefore, this paper recommends the use of electronic packages with component to solder elastic moduli ratio higher than 2 maintained with high component to solder and PCB to solder elastic thickness ratio for lowest bending-induced stresses.

Figure 7- 9 represent the effect of E_3/E_2 on the middle layer top and bottom stresses. From all figures, middle layer top stresses are the highest for E_3/E_2 values between 0 and 2 especially for unity E_3/E_2, h_1/h_2 and h_3/h_2 ratios. Also, top surface stresses are reduced for higher elastic moduli and thickness ratios. For E_3/E_2 values less than 2, bottom surface stress are observed to be very high while they vanish for higher ratiosE_3/E_2. For these reasons, electronic packages with very high component to solder and PCB to solder elastic moduli as well as thickness ratios are highly recommended.

Figure 10 – 15depict the effect of h_1/h_2 and h_3/h_2 ratios on middle beam layer stresses. From Figure 10 - 12, it can be clearly seen that top and bottom surfaces of the middle layer stresses vanish for $h_1/h_2 > 2$ and $h_3/h_2 > 5$ respectively. In contradiction, stress of the middle layer at the top and bottom interfaces vanish for $h_1/h_2 > 5$ and $h_3/h_2 > 2$, respectively, as presented in Figure 13 - 15. Therefore, it is highly recommended to build electronic structures with high component to solder and PCB to solder thickness ratios to ensure lowest mechanical stresses.

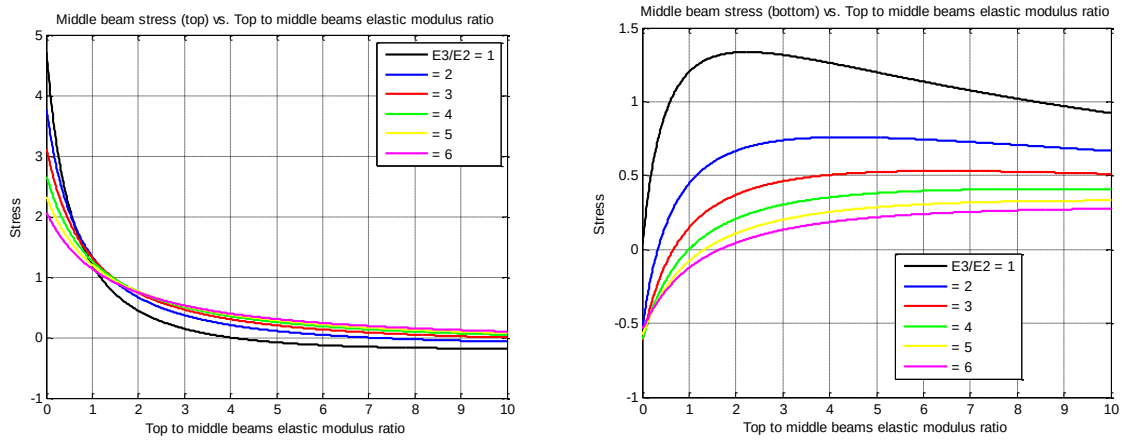

Figure 4. Middle beam stresses at the (left) top and (right) bottom surfaces as a function of top to middle beams elastic moduli ratios (E_1/E_2) at different bottom to middle beams elastic moduli ratios (E_3/E_2).

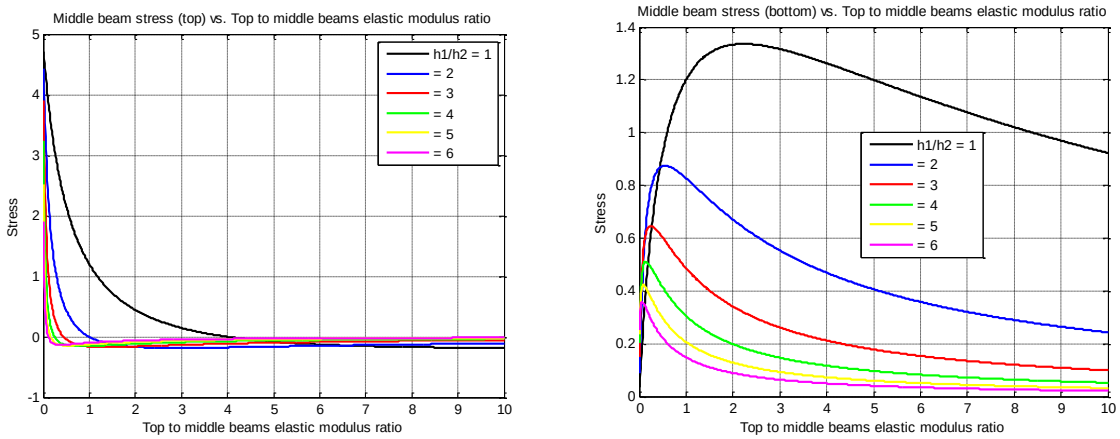

Figure 5. Middle beam stresses at the (left) top and (right) bottom surfaces as a function of top to middle beams elastic moduli ratios (E_1/E_2) at different top to middle beams thickness ratios (h_1/h_2).

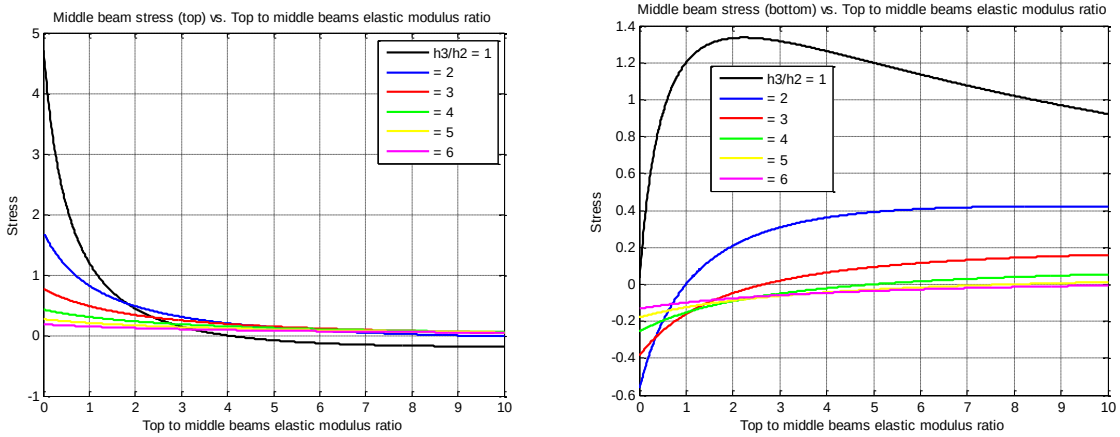

Figure 6. Middle beam stresses at the (left) top and (right) bottom surfaces as a function of top to middle beams elastic moduli ratios (E_1/E_2) at different bottom to middle beams thickness ratios (h_3/h_2).

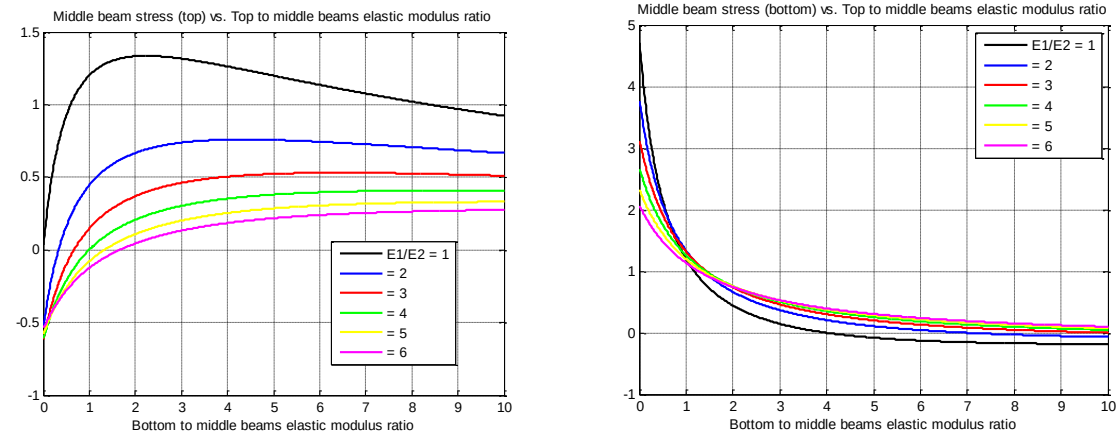

Figure 7. Middle beam stresses at the (left) top and (right) bottom surfaces as a function of bottom to middle beams elastic moduli ratios (E_3/E_2) at different top to middle beams elastic moduli ratios (E_1/E_2).

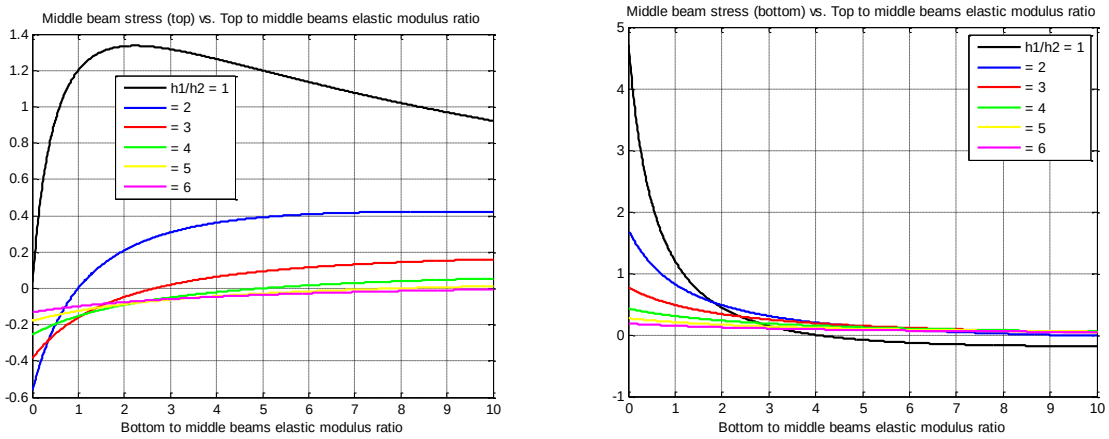

Figure 8. Middle beam stresses at the (left) top and (right) bottom surfaces as a function of bottom to middle beams elastic moduli ratios (E_3/E_2) at different top to middle beams thickness ratios (h_1/h_2).

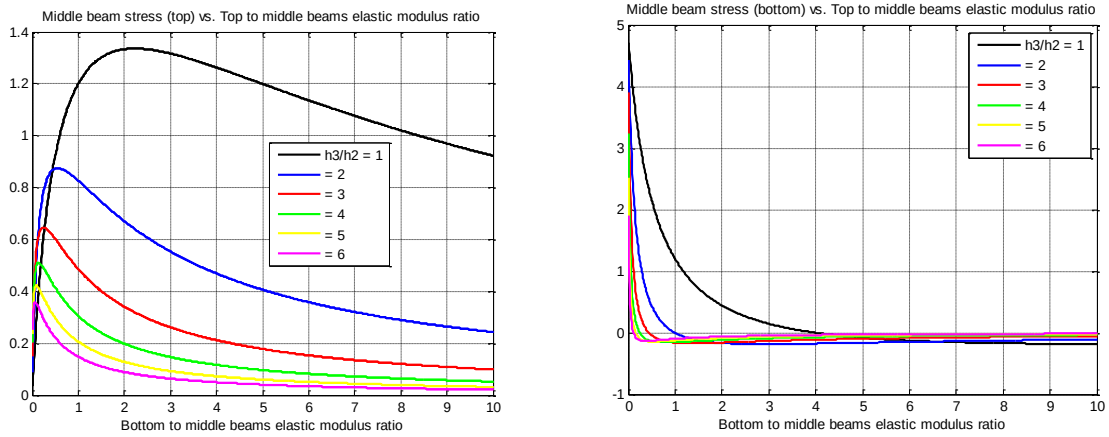

Figure 9. Middle beam stresses at the (left) top and (right) bottom surfaces as a function of bottom to middle beams elastic moduli ratios (E_3/E_2) at different bottom to middle beams thickness ratios (h_3/h_2).

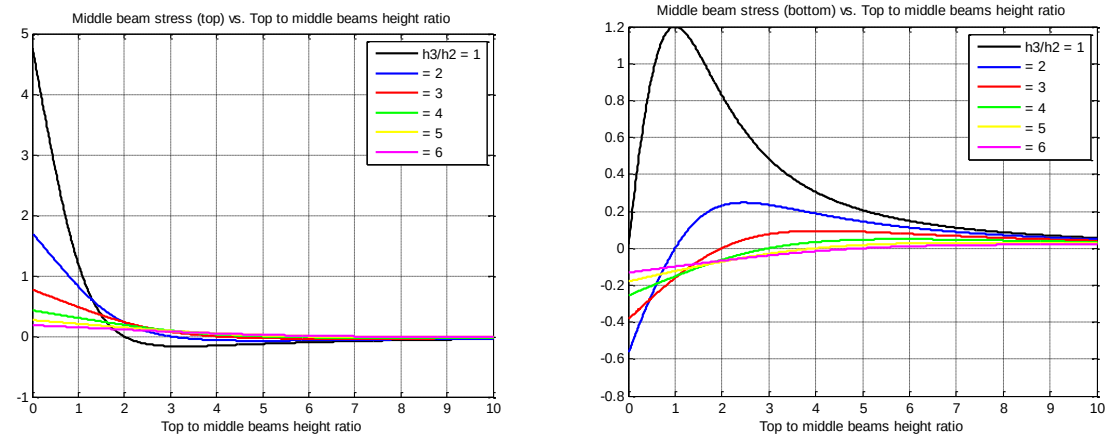

Figure 10. Middle beam stresses at the (left) top and (right) bottom surfaces as a function of top to middle beams height ratios (h_1/h_2) at different bottom to middle beams thickness ratios (h_3/h_2).

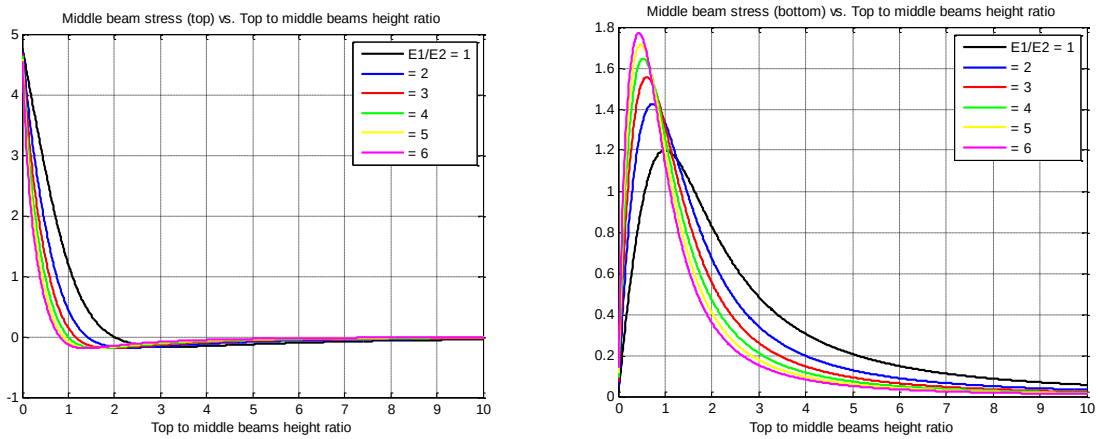

Figure 11. Middle beam stresses at the (left) top and (right) bottom surfaces as a function of top to middle beams height ratios (h_1/h_2) at different top to middle beams elastic moduli ratios (E_1/E_2).

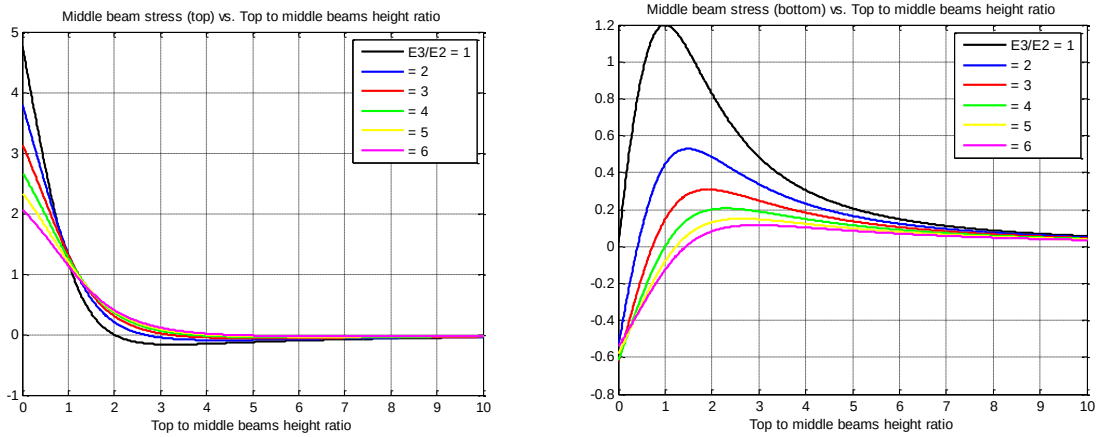

Figure 12. Middle beam stresses at the (left) top and (right) bottom surfaces as a function of top to middle beams height ratios (h_1/h_2) at different bottom to middle beams elastic moduli ratios (E_3/E_2).

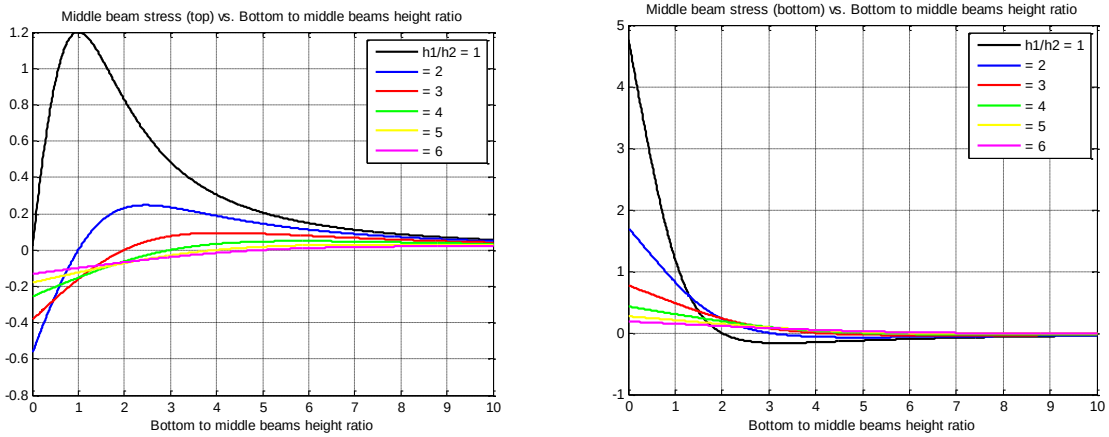

Figure 13. Middle beam stresses at the (left) top and (right) bottom surfaces as a function of bottom to middle beams height ratios (h_3/h_2) at different bottom to middle beams thickness ratios (h_3/h_2).

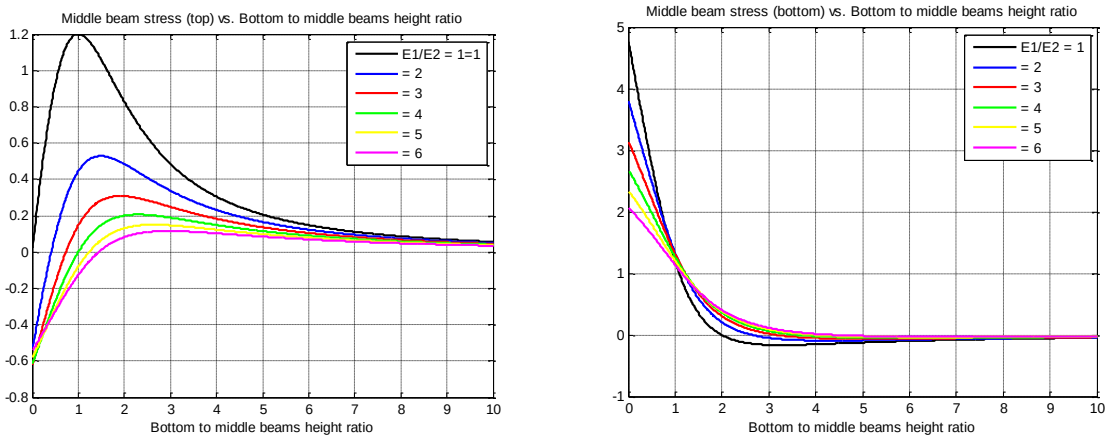

Figure 14. Middle beam stresses at the (left) top and (right) bottom surfaces as a function of bottom to middle beams height ratios (h_3/h_2) at different top to middle beams elastic moduli ratios (E_1/E_2).

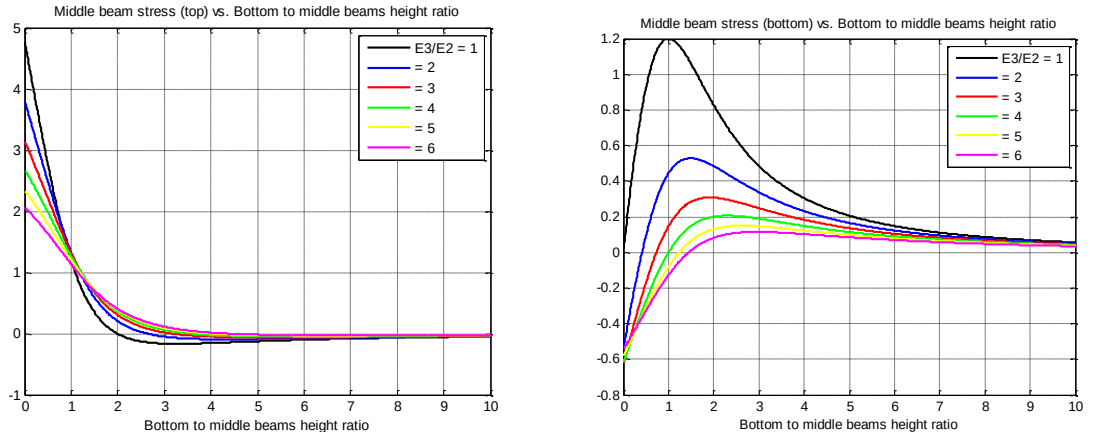

Figure 15. Middle beam stresses at the (left) top and (right) bottom surfaces as a function of bottom to middle beams height ratios (h_3/h_2) at different bottom to middle beams elastic moduli ratios (E_3/E_2).

6. Conclusions

This paper presented an experimental setup for the evaluation of a three-material composite beam lateral deflection. The materials of this beam were selected to be steel, aluminum and wood. Two bonding configurations were considered, glued and bolted. The experimentally measured lateral deflections of the composite beam were compared to theoretical calculations. The comparison showed that glued beam system is in a better agreement with theory than bolted configuration. In addition, the analytical solution of the three-material beam was extended to solve for the middle layer stresses. Finally, the effect of the key parameters of the composite beam on beam stresses is discussed in detail with emphasis on the application of structural analysis of electronic assemblies subjected to mechanical bending.

Acknowledgment

The authors wish to thank the deanship of scientific research at the Hashemite University for providing the necessary tools and funds. In addition, we would like to acknowledge Mr. Ahmad Al-Shorman of the mechanical engineering department of the Hashemite University for his good help throughout this work.

References

[1] Viest, I. M. (1960). Review of research on composite steel-concrete beams. Journal of the Structural Division, 86(6), 1-22.

[2] Suhir, E. (1988). On a paradoxical phenomenon related to beams on elastic foundation: Could external compliant leads reduce the strength of a surface-mounted device?. Journal of applied mechanics, 55(4), 818-821.

[3] Miklofsky, H. A., Brown, M. R., & Gonsior, M. J. (1962). Epoxy bonding compounds as shear connectors in composite beams. Engineering Research Series, 62-2.

[4] Kriegh, J. D., & Endebrock, E. G. (1963). THE USE OF EPOXY RESINS IN REINFORCED CONCRETE--STATIC LOAD TESTS: PART II (No. Final Report No. 2).

[5] Pitarresi, J. M., & Ceurter, J. (1999). Elasticly coupled beams loaded by a point force. In 13th Engineering Mechanics Conference, Baltimore, MD, June (pp. 13-16).

[6] Gharaibeh, M. A., Liu, D., & Pitarresi, J. M. (2017). A pair of partially coupled beams subjected to concentrated force. IEEE Transactions on Components, Packaging and Manufacturing Technology, 7(8), 1293-1304.

[7] Wong, E. H., Mai, Y. W., Seah, S. K., Lim, K. M., & Lim, T. B. (2007). Analytical solutions for interconnect stress in board level drop impact. IEEE transactions on advanced packaging, 30(4), 654-664.

[8] Wong, E. H., & Wong, C. K. (2009). Approximate solutions for the stresses in the solder joints of a printed circuit board

subjected to mechanical bending. International Journal of Mechanical Sciences, 51(2), 152-158.

[9] Stüssi F., Zusammengesetzte Vollwandträger (Composed Beams), International Association for Bridge and Structural Engineering (IABSE), 1947, 8, 249-269

[10] Newmark, N. M. (1951). Test and analysis of composite beams with incomplete interaction. Proceedings of society for experimental stress analysis, 9(1), 75-92.

[11] Lee, P. G., Shim, C. S., & Chang, S. P. (2005). Static and fatigue behavior of large stud shear connectors for steel–concrete composite bridges. Journal of constructional steel research, 61(9), 1270-1285.

[12] Gharaibeh, M. A., Su, Q. T., & Pitarresi, J. M. (2016). Analytical solution for electronic assemblies under vibration. Journal of Electronic Packaging, 138(1).

[13] Gharaibeh, M. A. (2018). Reliability analysis of vibrating electronic assemblies using analytical solutions and response surface methodology. Microelectronics Reliability, 84, 238-247.

[14] Gharaibeh, M. (2018). Reliability assessment of electronic assemblies under vibration by statistical factorial analysis approach. Soldering & Surface Mount Technology.

[15] Gharaibeh, M. A., Su, Q. T., & Pitarresi, J. M. (2018). Analytical model for the transient analysis of electronic assemblies subjected to impact loading. Microelectronics Reliability, 91, 112-119.

[16] Gharaibeh, M. A., & Pitarresi, J. M. (2019). Random vibration fatigue life analysis of electronic packages by analytical solutions and Taguchi method. Microelectronics Reliability, 102, 113475.

[17] Gharaibeh, M. A. (2020). Analytical solutions for electronic assemblies subjected to shock and vibration loadings. In Handbook of Materials Failure Analysis (pp. 179-203). Butterworth-Heinemann.

[18] Ghadiri, M., Malekzadeh, K., & Ghasemi, F. A. (2015). Free Vibration of an Axially Preloaded Laminated Composite Beam Carrying a Spring-Mass-Damper System with a Non-Ideal Support. Jordan Journal of Mechanical & Industrial Engineering, 9(3).

[19] Sari, M. E. S., & Al-Qaisia, A. (2016). Nonlinear Natural Frequencies and Primary Resonance of Euler-Bernoulli Beam with Initial Deflection using Nonlocal Elasticity Theory. Jordan Journal of Mechanical & Industrial Engineering, 10(3).